Lightning Phenomenology Notes

Note 13

30 October 1984

RETURN-STROKE TRANSMISSION-LINE MODEL

C. E. Baum
Air Force Weapons Laboratory

L. Baker
Mission Research Corporation

ABSTRACT

The transmission-line model previously developed for the leader stroke is applied to the return-stroke of a lightning channel. The charge stored in the corona is converted into current by a discharge wave. The dependence of propagation velocity on coronal charge and radius leads to front steepening and the development of a jump discontinuity or electromagnetic shock in a finite time.

CONTENTS

ILLUSTRATIONS

I. INTRODUCTION

Despite a half-century of investigation of lightning through optical and electromagnetic means, the basic physics of much of the discharge process is still poorly understood. Fundamental parameters such as the diameter of the lightning discharge are the subject of continued controversy. For this reason it is of value to construct simple models of lightning in order to estimate the observable consequences of presumed physical mechanisms. What is proposed here is one such model.

It is reasonable to study the basic physics of the return stroke as a means of first gaining some understanding of lightning channel properties, and then using the information deduced to attack the more difficult problem of the lightning leader. As Uman [1] remarked, "while the time might not yet be ripe for a theoretical description of the stepped leader, there are many lightning problems that would appear to be amenable to analysis... [including] the dart leader and return-stroke wave-front propagation." The theoretical model to be described here implies the existence of an observable corona with a radius of the order of a few meters and explains a number of features of lightning return-strokes. It should therefore be of interest as it not only explains observed behavior but should be testable.

II. RETURN-STROKE MODEL: BACKGROUND

Our model treats the lightning channel as a transmission line. Such models have a long history [2, 3, 4]. Experiment and theory suggest that wire transmission lines at high voltages are surrounded by corona discharges [5, 6] that substantially affect their properties. The lightning transmission-line model of Baum [7] is a development and application of the corona-surrounded transmission-line model presented in [5]. It is assumed that during leader advance charge is deposited in the corona surrounding the lightning channel. There is optical evidence for a substantial corona with a typical diameter of a few meters [8, 9], although there is controversy over the effects of atmospheric scattering and film characteristics on the interpretation of this evidence.

Salanave [10] presents a photograph and its enlargement which appears to show a corona discharge about a lightning channel. His Figure 7.6 implies a scale of about 15 cm for the arc channel radius and 0.75 m radius for the visible portion of the corona. The actual corona may be larger, with the more diffuse current in the outer regions not registering on the film. Wagner [11] takes a corona radius of about 3 m. Uman [9] says "luminous stepped-leader diameters have been measured photographically to be between 1 and 10 m .... the large luminous diameter is [thought to be] due to a corona sheath surrounding the core." If we assume the coronal radius at the time of the return stroke is unchanged, and that atmospheric scattering and film fogging may be ignored, this suggests a coronal radius of 0.5-5 m. Berger [12] estimates the coronal radius as about 6 m with a charge per unit length 10^{-3} C m^{-3} using 3 MV/m as the static breakdown field of air. He also states: "the diameter of the corona shell has never been measured .... Approximate values may vary from a few meters to 20 or 40 m." A more complete theory of the corona discharge is needed if we are to determine the charge, current density, and optical emission as a function of radius.

The return stroke is assumed to be the consequence of this stored charge being converted into a current by a discharge wave travelling up the line. This return-stroke model is therefore a departure from the others [2, 3] in that we do not assume an initially uncharged line which passively transmits a current supplied at one end, but rather a charged line which supplies the current itself. Wagner and Hileman [13] considered a rapidly collapsing corona about a return stroke, and Pierce [14] and Rao and Bhattacharya [15] considered a slowly collapsing corona as providing the "continuing current" between return strokes. Wagner [11] viewed the return stroke as neutralizing the charge laid down by the leader.

The table on page 19 of [7] shows some of the relations among the corona radius Ψ_c, the velocity v, the charge per unit length Q', and the current I for a leader pulse which corresponds to an expanding corona. The return stroke, however, corresponds to a collapsing corona which, as will be seen, has some quite different characteristics. Considering a simple constant velocity wave with

$$\Psi_c = \frac{|Q'|}{2\pi\varepsilon_0 E_b}$$

$$E_b \approx 2 \text{ MV/m}$$

$$|I| = |Q'|v$$

$$\frac{v}{c} \approx \frac{1}{3} \qquad (1)$$

one can take various observations of current and imply Q' and Ψ_c. Using the data of Garbagnati [17] and Berger [28] the distribution of lightning return-stroke currents cuts off above about 100 kA. This corresponds to

$$|I| \approx 100 \text{ kA}$$

$$|Q'| \approx 1 \text{ mC/m}$$

$$\Psi_c \approx 9 \text{ m} \qquad (2)$$

A 14 Km long lightning channel, for example [16] would corresponds to 14 C of stored charged, which is roughly the observed maximum charge delivered. These numbers represent approximate maxima and typical Q', I, and hence Ψ_c are somewhat smaller.

As we develop our return-stroke model, let us keep these general magnitudes in mind.

III. NONLINEAR TRANSMISSION-LINE MODEL

The basic transmission line geometry is sketched in fig. 1 (reproduced from [7]). The return path of the transmission line is treated as a cylindrical return path at large radius, Ψ_∞. It is shown in [18] that this is a reasonable approximation for the line properties (treating the channel as a thin wire antenna) so long as Ψ_c is small compared to the wavelength considered. Strictly speaking, we would in general have a frequency-dependent inductance, etc. The dependence is as the logarithm of the wavelength and is therefore a weak function of frequency. The accurate treatment of this effect would introduce a major complication in the model, requiring a treatment in frequency space followed by a transform back to time domain. The model treated here should be reasonable over a limited frequency range, but we should bear in mind the dispersive nature of transmission along such a line due to the frequency dependence of the line parameters which is neglected here. We use the same notation of [7], retaining primes on the quantities that are per unit length.

The line equations are:

$$\frac{\partial}{\partial z}\left(\frac{Q'}{C'}\right) = -L' \frac{\partial I}{\partial t} \tag{3}$$

$$\frac{\partial I}{\partial z} = -\frac{\partial Q'}{\partial t} \tag{4}$$

where the voltage may be found from the fundamental relation $V = Q'/C'$, where Q' is the charge per unit length. We have neglected the leakage capacitance in the corona, i.e., the resistor is assumed to be of negligible resistance or large conductance G_c' so that the time constant C_c'/G_c' is small compared to times of interest and the voltage across C_c' can be neglected. Note, however, that we still assume that the conducting core of radius Ψ_0 is of sufficiently high conductivity such that it carries essentially all the current in the z direction (longitudinal). Furthermore, the corona conductivity is assumed to be not so large as to

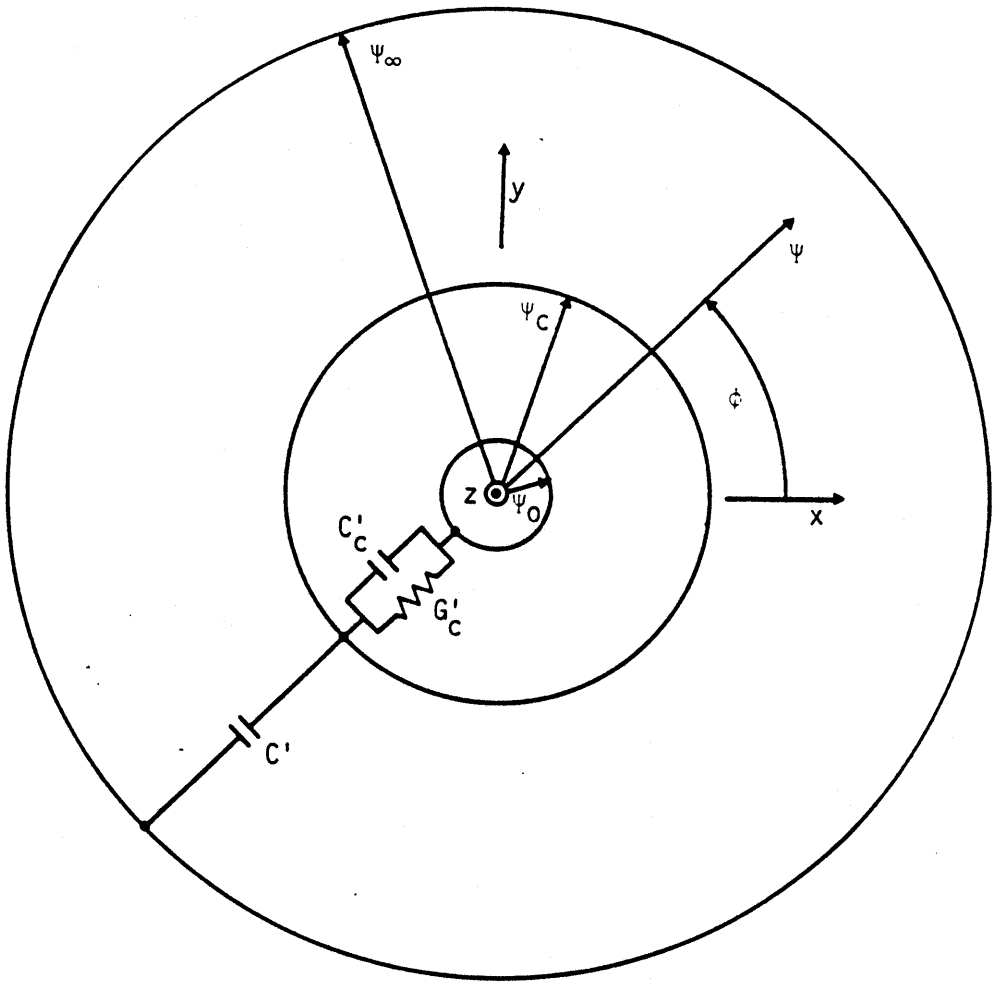

Figure 1. Sketch of the assumed transmission-line geometry of the model. A cross-sectional view is shown.

prevent diffusion of magnetic field through the corona (skin effect) during times of interest. Reference 7 gives the values for the inductance L' and capacitance C' per unit length, the latter being a function of Q' due to the existence of a corona whose radius depends upon Q'. We assume that the corona extends out from the channel until the field is less than E_b = 2 MV/m, giving the condition on corona charge and radius:

$$|Q'| = 2\pi \varepsilon_0 E_b \Psi_c \tag{5}$$

This gives a nonlinear transmission line equation (since C' is a function of Q') which may be solved [7, 19] as

$$Q' = Q'(\tau)$$

$$\tau = t \pm z/v(Q')$$

$\left\{\begin{matrix}\text{top}\\ \text{bottom}\end{matrix}\right\}$ sign corresponds to propagation in $\left\{\begin{matrix}-z\\ +z\end{matrix}\right\}$ direction

$$v = \sqrt{\frac{1}{L'} \frac{d}{dQ'} \left(\frac{Q'}{C'}\right)} \tag{6}$$

where v is the propagation velocity of the potential wave.

The wave velocity divided by the speed of light is [7]

$$\frac{v}{c} = \beta = \sqrt{\frac{\ell n\left(\frac{Q'_\infty}{e|Q'|}\right)}{\ell n\left(\frac{Q'_\infty}{Q'_0}\right)}} \tag{7}$$

where Q'_∞ and Q'_0 are related to Ψ_∞ and Ψ_0 in the same manner as Q'_c is related to Ψ_c:

$$Q'_\infty = 2\pi\varepsilon_0 E_b \Psi_\infty$$

$$Q'_0 = 2\pi\varepsilon_0 E_b \Psi_0 \tag{8}$$

Fig. 2 shows β as a function of the normalized charge on the line. Note that the wave velocity is limited by the velocity when the corona radius has shrunk to the channel radius, and is slightly less than c, the maximum value of β being:

$$\beta^2 = 1 - \frac{1}{\ell n\left(\frac{\Psi_\infty}{\Psi_0}\right)} \tag{9}$$

If we used a more complex formula for the corona radius which did not allow the corona to contract beyond Ψ_0, i.e., if the derivate of the coronal radius (and hence the derivative of the capacitance per unit length) vanished near the arc radius, we would regain the limiting wave velocity of the speed of light. Note also that the normalized wave velocity is related to the three radii (channel, corona, return) by the expression:

$$\Psi_c = \frac{\Psi_\infty^{1-\beta^2}\left(\Psi_0^{\beta^2}\right)}{e} \tag{10}$$

This follows from (6.3) of [7] or (7) above,

$$\beta^2 = \frac{\ell n\left(\frac{\Psi_\infty}{e\Psi_c}\right)}{\ell n\left(\frac{\Psi_\infty}{\Psi_0}\right)} \tag{11}$$

which gives immediately

$$\left(\frac{\Psi_\infty}{\Psi_0}\right)^{\beta^2} \quad \left(\frac{\Psi_\infty}{e\Psi_c}\right) \tag{12}$$

and (10) when solved for Ψ_c. Since β is typically in the range 0.1 to 0.5 for return strokes, it is clear that the coronal radius is insensitive to the arc radius but relatively sensitive to the return current radius.

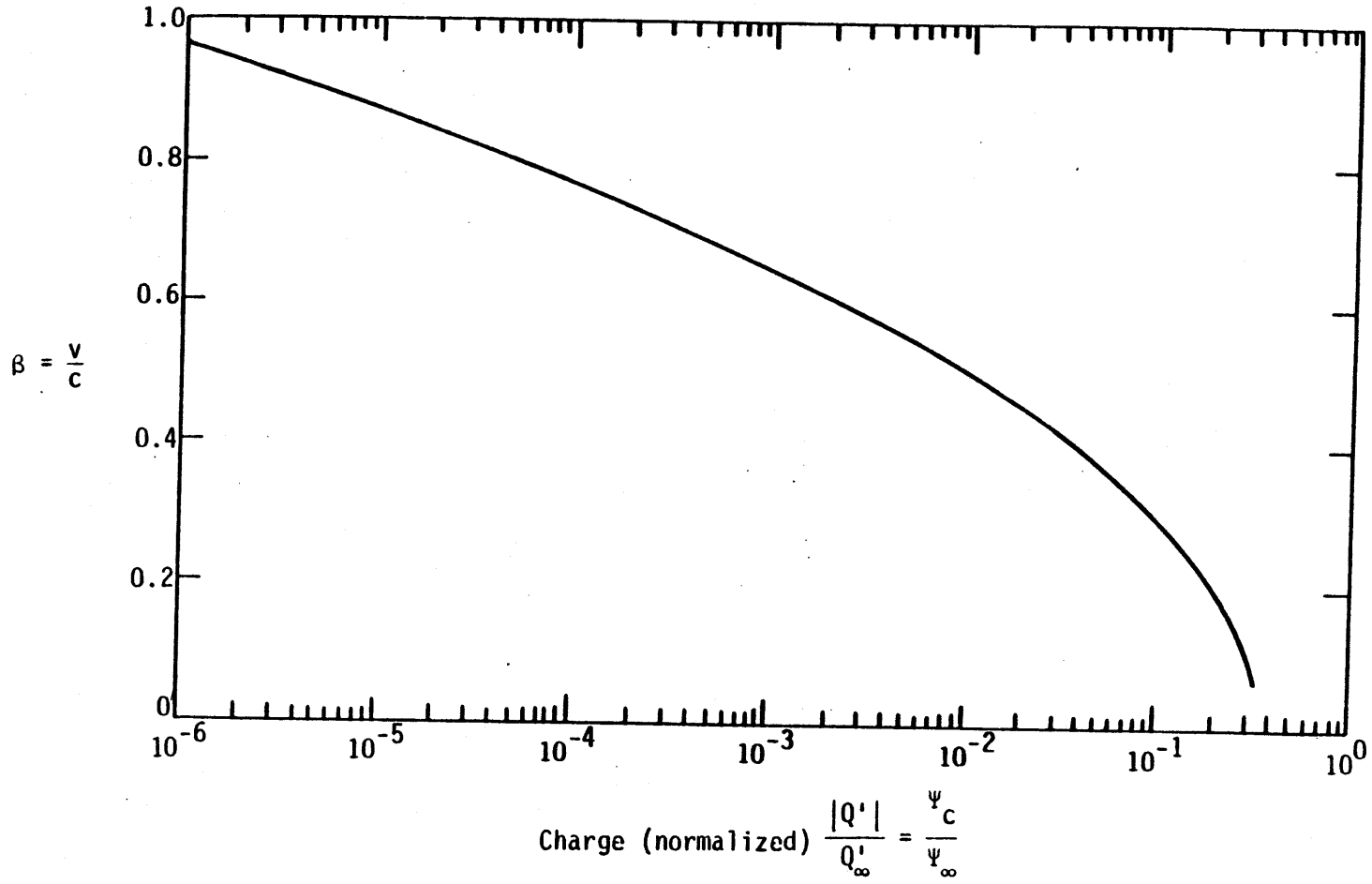

Figure 2. Wave velocity as a fraction of the speed of light c, as a function of the normalized charge $|Q'|/Q'_\infty$ or normalized corona radius, Ψ_c/Ψ_∞.

The transmission-line equations given above may be integrated to give the current and other variables of physical interest as a function of charge per unit length. The current is governed by the differential equation which (in terms of the new variable τ) is

$$\frac{\partial I}{\partial \tau} = \mp v(Q'(\tau)) \frac{\partial Q'}{\partial \tau} \tag{13}$$

which may be immediately integrated as

$$I - I_i = \mp \int_{Q_i'}^{Q'} v(q)\, dq \tag{14}$$

where we have

$$\left.\begin{aligned} I_i &= I(\tau_i) \\ Q_i' &= Q'(\tau_i) \end{aligned}\right\} \quad \text{initial conditions at } \tau = \tau_i \tag{15}$$

With the change of variables $y = \sqrt{\ell n(Q_\infty'/e|Q'|)}$ we find:

$$I = I_i \pm \text{sign}(Q') \frac{2cQ_\infty'}{e} \left[\ell n\left(\frac{Q_\infty'}{Q_0'}\right)\right]^{-1/2} \int_{\sqrt{\ell n(Q_\infty'/e|Q_i'|)}}^{\sqrt{\ell n(Q_\infty'/e|Q'|)}} y^2 e^{-y^2}\, dy \tag{16}$$

which by inspection shows that the current is of one sign (does not "overshoot") and is in fact monotonic in $|Q'|$ (increasing or decreasing, but not both) since the integrand is positive semi-definite. With no initial current:

$$I = \pm \text{sign}\,(Q') \left[\frac{2cQ_\infty'}{e} \ell n\left(\frac{Q_\infty'}{Q_0'}\right)\right]^{-1/2} \left\{ \frac{e|Q_i'|}{2Q_\infty'} \ell n\left(\frac{Q_\infty'}{e|Q_i'|}\right) - \frac{e|Q'|}{2Q_\infty'} \ell n\left(\frac{Q_\infty'}{e|Q'|}\right) \right.$$

$$\left. + \frac{\sqrt{\pi}}{4} \text{erf}\left[\ell n\left(\frac{Q_\infty'}{e|Q'|}\right)\right]^{1/2} - \frac{\sqrt{\pi}}{4} \text{erf}\left(\left[\ell n\left(\frac{Q_\infty'}{e|Q_i'|}\right)\right]^{1/2}\right) \right\} \tag{17}$$

the error function, erf(x), is defined in [20]. We shall assume that the initial charge per unit length on the line $|Q'_i|$ is Q'_∞/e, the maximum value allowed by this model [7], and corresponds to a a vanishing wave propagation velocity. It is plausible that the channel corona will charge up to this value, whereupon further changes cannot propagate effectively. Under this condition we have

$$I = \pm \text{sign}\,(Q') \frac{2cQ'_\infty}{e}\left[\ell n\left(\frac{Q'_\infty}{Q'_0}\right)\right]^{-1/2}\left\{-\frac{e}{2}\frac{Q'}{Q'_\infty}\left[\ell n\left(\frac{Q'_\infty}{e|Q'|}\right)\right]^{1/2}\right.$$

$$\left. + \frac{\sqrt{\pi}}{4}\,\text{erf}\left(\left[\ell n\left(\frac{Q'_\infty}{e|Q'|}\right)\right]^{1/2}\right)\right\} \qquad (18)$$

In the limit where all of the corona charge is removed from the corona by the passage of the wave, $|Q'| = Q'_0$, the current is maximized in magnitude. This is plotted in fig. 3. Note the nonmonotonic dependence of the maximum current on Q'_0. This may be seen in some of the figures below which plot the spatial dependence of the current. The maximum of $|I|e2cQ'_\infty$ is for $Q'_\infty/Q'_0 = 45.1$ (see Table 1), and I vanishes at $Q'_\infty/Q'_0 = e$.

In evaluating the electromagnetic signal produced, the following quantity [21] is of interest:

$$\vec{T} = \frac{\partial}{\partial t}\int_{V'} \vec{J}(r',t)\, dV' \qquad (19)$$

This "effective source vector" $\vec{T}$ is related to the far electric field, for example, by

$$E(t) = -\frac{\mu}{4\pi r}\vec{1}_t \cdot \vec{T}(t - r/c) \qquad (20)$$

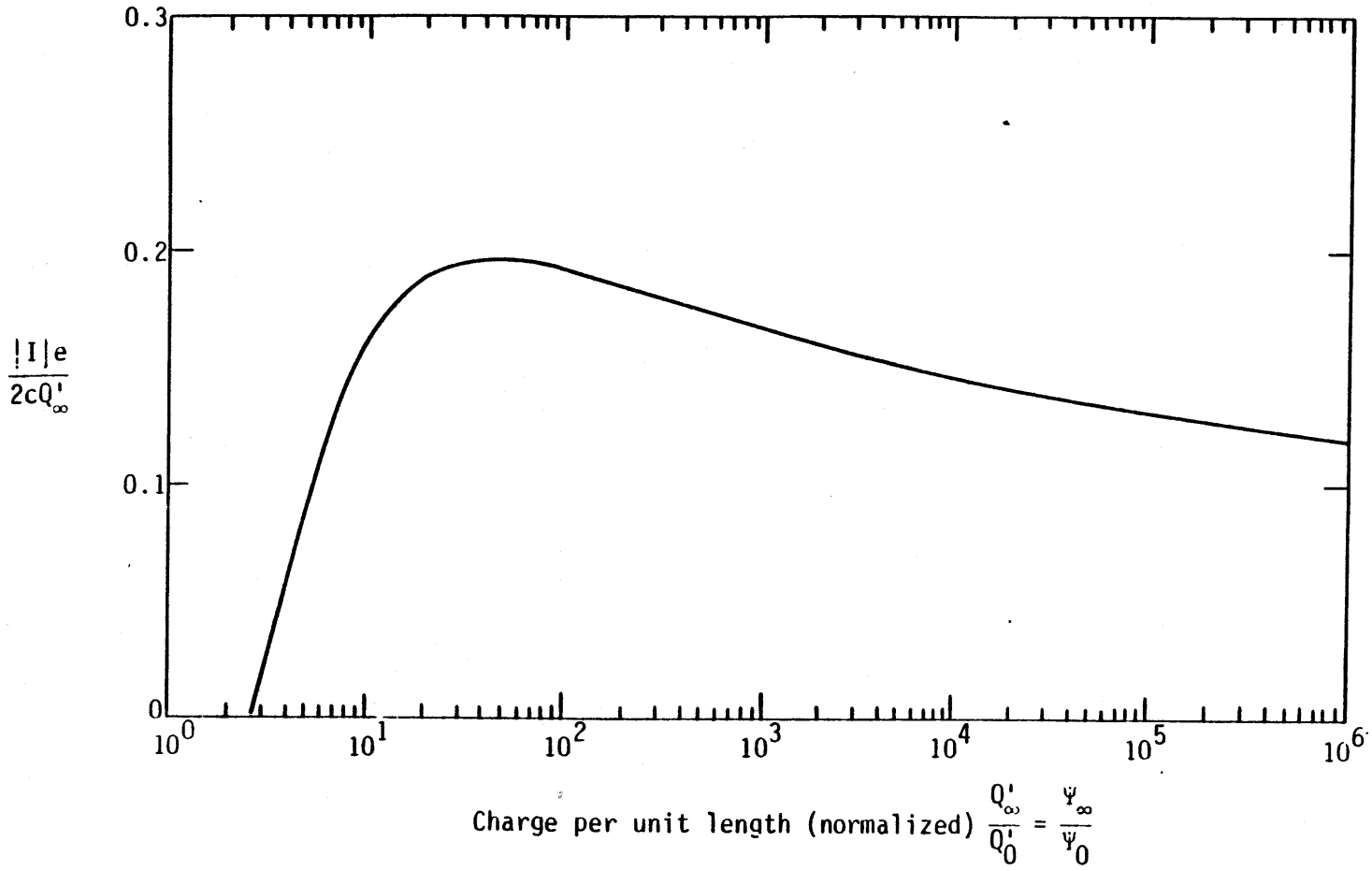

Figure 3. Maximum Current as a Function of $\frac{Q'_\infty}{Q'_0} = \frac{\Psi_\infty}{\Psi_0}$.

TABLE 1. CRITICAL VALUES OF Q'_∞/Q'_0

$\frac{Q'_\infty}{Q'_0}$	Significance	β (Shock)	$\frac{\lvert I\rvert e}{2cQ'_\infty}$ I (Shock Solution)	$\frac{\lvert I\rvert e}{2cQ'_\infty}$ I (Continuous Solution)
11.96	Minimum for shock solution	0	0	0.1695
45.10	Maximum I (continuous)	0.4061	0.1908	0.1971
57.79	I (continuous) = I (shock)	0.4127	0.1966	0.1966
86.74	Maximum β	0.4160	0.2015	0.1942
123.2	Maximum I (shock)	0.4142	0.2025	0.1909

(see [20] for a complete discussion). The vector $\vec{T}$ is essentially the vector $\vec{q}$ of Becker [22], and is a generalization of the "radiation vector" $\vec{N}$ of Schelkunoff and Friis [18] to nonsinusoidal currents. By interchanging the order of integration and differentiation, and integrating the part of the arc for which $z > 0$:

$$T_0(t) = \int_{z=0}^{z=\infty} \frac{\partial I}{\partial t}\bigg|_z dz \tag{21}$$

With the substitution

$$\frac{\partial I}{\partial t}\bigg|_z = \frac{dI(\tau)}{d\tau}\frac{\partial \tau}{\partial t}\bigg|_z$$

we use the similarity solution (6) above with

$$\tau = t - z/v(Q'),$$

where $Q' = Q'(\tau)$. From [7] we find

$$\frac{\partial \tau}{\partial t}\bigg|_z = -\frac{1}{v}\left\{1 + z\frac{d}{d\tau}\left[\frac{1}{v}\right]\right\}^{-1}$$

Thus

$$T_0(t) = -\int_{z=0}^{z=\infty} \frac{dI(\tau)}{d\tau}\ \frac{1}{v}\left\{1 + z\,\frac{d}{d\tau}\left[\frac{1}{v}\right]\right\}^{-1} dz \qquad (22)$$

This may be converted to an integral over τ via

$$d\tau\Big|_t = \frac{-dz}{v}\left\{1 + z\,\frac{d}{d\tau}\left[\frac{1}{v}\right]\right\}^{-1}$$

which follows from $\tau = t - z/v(Q')$ [7]. Thus

$$T_0(t) = \int_{\tau=-\infty}^{\tau=t} \frac{dI(\tau)}{d\tau}\ v(Q')d\tau$$

$$= \int_0^I v\ dI(\tau) = \int_{Q'(-\infty)}^{Q'(t)} v\,\frac{dI}{dQ'}\,dQ' = \int_{Q'(-\infty)}^{Q'(t)} v^2(Q')\ dQ'$$

$$= \frac{c^2}{\ell n(Q'_\infty/Q'_0)} \int_{Q'(-\infty)}^{Q'(t)} \ell n(Q'_\infty/e|Q'|)\ dQ'$$

$$= -\text{sign}\ (Q')\ \frac{c^2 Q'_\infty}{\ell n\left(\frac{Q'_\infty}{Q'_0}\right)}\left[\frac{Q'}{Q'_\infty}\,\ell n\,\frac{Q'}{Q'_\infty} - \frac{Q'(-\infty)}{Q'_\infty}\,\ell n\left(\frac{Q'(-\infty)}{Q'_\infty}\right)\right] \qquad (23)$$

If we assume that the initial charge on the line is $Q'(-\infty) = Q_\infty/e$, we have:

$$T_0 = -\text{sign}\ (Q')\ \frac{c^2 Q'_\infty}{e\ \ell n(Q'_\infty/Q'_0)}\left[1 + \frac{e|Q'|}{Q'_\infty}\,\ell n\,\frac{|Q'|}{Q'_\infty}\right] \qquad (24)$$

The source T_0 is plotted in fig. 4 as a function of $|Q'|/Q'_\infty$ for fixed Q'_∞/Q'_0 for any $t - r/c$ in (20), Q' may be found and then T_0.

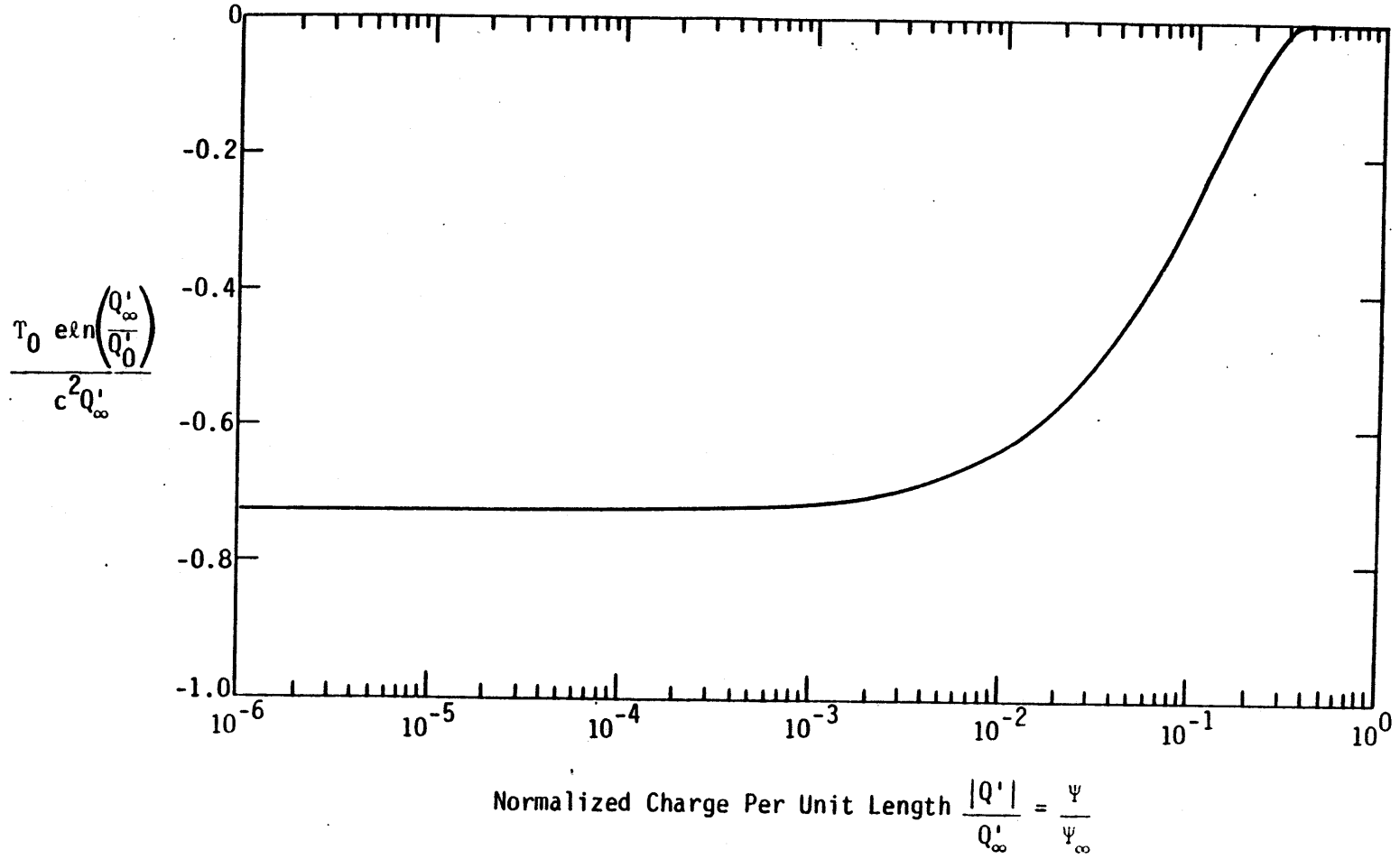

Figure 4. Effective radiation source vector amplitude Υ verus $|Q'|/Q'_\infty$.

As discussed in Section 5, eventually an electromagnetic shock forms. How soon it forms depends on our assumption of the form of $0'(t)$ at $z = 0$. After the shock forms the above solution does not apply.

The effective T_{eff} differs from T_0 due to the boundary conditions. A perfectly conducting ground produces an image field. Thus, for a return stroke initiated at ground level, $T_{eff} = 2T_0$. If the stroke initiates with attachment above ground level, at early times there are two waves along the channel, propagating up and down from the point of attachment. The total field would then be due to the sum of all of these waves and their images. This could result in a T_{eff} as large as $4T_0$, at least until the downward propagating wave met its image wave at the surface. Here cancellation would occur for this pair of waves. Note also that T must only be used, as in (17), in the far radiation zone for which the size of the radiating volume containing the lightning stroke is small compared to the distance between the observer and the stroke. Otherwise, the variation in phase of the contribution of different portions of the channel must be considered.

IV. ELECTROMAGNETIC SHOCK LIMIT

We will show below that the wave tends to form a jump or "shock". This is to be expected because the wave velocity increases as charge is removed from the corona and the corona radius shrinks. This causes a trailing disturbance to catch up to the wave front. The situation in then qualitatively as in a shock wave in a gas, for which the shock front is subsonic with respect to flow behind it. Just as acoustic waves steepen into shocks as a consequence, waves in this model steepen into discontinuous jumps in a finite length of time. We may then treat jump conditions analagous to the Rankine-Hugoniot jump conditions for the "shock" solution discussed in [7].

Conservation of charge gives a jump condition

$$I(\text{behind}) - I(\text{ahead}) = v[Q'(\text{behind}) - Q'(\text{ahead})] \tag{25}$$

where [26]

$$I(\text{ahead}) = 0,\ \left|Q'(\text{ahead})\right| = Q'(-\infty) = Q'_\infty/e,\ \left|Q'(\text{behind})\right| = Q'_0 \tag{26}$$

which is generally negligible compared to Q'(ahead). The fundamental relation for energy conservation is [21, p. 48]

$$\frac{\partial w}{\partial t} + \nabla \cdot \vec{S} = 0\ ,\ w = \frac{1}{2}\left[\varepsilon_0 \vec{E} \cdot \vec{E} + \mu_0 \vec{H} \cdot \vec{H}\right]\ ,\ \vec{S} = \vec{E} \times \vec{H} \tag{27}$$

where w is the electromagnetic energy (per unit volume) and $\vec{S}$ the Poynting flux vector. Integrating over a cylindrical volume containing the wave and using Gauss' law:

$$\int_V \frac{\partial w}{\partial t}\, dV + \int_A \vec{S} \cdot d\vec{A} = 0 \tag{28}$$

Shrinking the length of the cylindrical pillbox down to zero we neglect the cylindrical surface and have only the flux contributions on the planar surfaces ahead and behind the front, with:

$$P = \int_A \vec{S} \cdot d\vec{A} = 2\pi \int_0^{\Psi_\infty} S_z \, \Psi d\Psi \tag{29}$$

$$\int_V \frac{\partial w}{\partial t} \, dV + P(\text{ahead}) - P(\text{behind}) = 0 \tag{30}$$

where P is the power in our transmission-line model. We use the identity:

$$\int_V \frac{\partial w}{\partial t} \, dV = \frac{d}{dt} \int_V w dV \tag{31}$$

In a frame co-moving with the front the operator $d/dt \equiv \partial/\partial t + \vec{v} \cdot \nabla$ becomes simply $\vec{v} \cdot \nabla$ for a steady wave, and we have finally

$$v[W'(\text{ahead}) - W'(\text{behind})] + P(\text{ahead}) - P(\text{behind}) = 0 \tag{32}$$

where W' is the energy per unit length in our transmission-line model. This gives us a final relation between I and v. Note that dissipative effects, such as the resistive losses required to establish an arc, are neglected (unlike the treatment for a hydrodynamic shock, which is irreversible).

Ahead of the front W' is the electrostatic energy per unit length due to the electric field between Ψ_∞ and Ψ_c, the contribution within being relatively small compared to this term (and would require a detailed model for the charge distribution in the corona for its evaluation). Then

$$W'(\text{ahead}) = \frac{Q'^2_{(-\infty)}}{4\pi\varepsilon_0} \ell n \left(\frac{Q'_\infty}{|Q'|} \right) = \frac{Q'^2_{(-\infty)}}{4\pi\varepsilon_0} \ell n \left(\frac{\Psi_\infty}{\Psi_c} \right) \tag{33}$$

The expression for W'(behind) contains a similar term along with a magnetic energy term due to the current along the channel.

$$W'(\text{behind}) = \frac{\mu_0}{4\pi} I^2 \ell n\left(\frac{\Psi_\infty}{\Psi_0}\right) + \pi\varepsilon_0 \Psi_c^2 E_b^2 \ell n\left(\frac{\Psi_\infty}{\Psi_c}\right) \tag{34}$$

while the radial electric field and azimuthal magnetic field gives an axially directed Poynting vector

$$P(\text{ahead}) = \frac{-Q_c' I}{2\pi\varepsilon_0} \ell n\left(\frac{\Psi_\infty}{\Psi_c}\right) \tag{35}$$

Now assuming that most of the available charge is depleted behind the front so that $\Psi_c \simeq \Psi_0 \ll \Psi_\infty$ and E outside Ψ_c is very small, P(behind) $\simeq$ 0.

Solving for I, the jump in current, gives for $|Q'| = Q_0'$

$$I = \frac{cQ_\infty'}{e\sqrt{\ell n(Q_\infty'/Q_0')}} \sqrt{1 - \frac{Q_0' 2e}{Q_\infty'} \ell n\left(\frac{Q_\infty'}{Q_0'}\right) + \frac{Q_0'^2 e^2}{Q_\infty'^2} \ell n\left(\frac{Q_\infty'}{Q_0'}\right)} \simeq \frac{cQ_\infty'}{e\sqrt{\ell n(Q_\infty'/Q_0')}} \tag{36}$$

and

$$\beta = \frac{v}{c} = \frac{Ie}{c(Q_\infty' - Q_0' e)} \simeq \frac{1}{\sqrt{\ell n(Q_\infty'/Q_0')}} \tag{37}$$

where in (34) we have neglected Q_0' relative to Q_∞'/e. We have plotted the approximate β and I in fig. 5. By comparing figs. 3 and 5 it may be seen that the current asymptotes to the jump current value for large changes in charge, as one would expect. In the shock limit, the radiation field contribution (that contribution to the electric and magnetic fields which falls off as 1/r) is due to processes near the front only, as the current behind rapidly approaches the constant value of the jump current I. The τ vector defined above may be found by using the shock front velocity (34) in (22), obtaining

$$\tau(t) = \frac{c^2(Q_\infty' - Q_0')}{\ell n(Q_\infty'/Q_0')} \tag{38}$$

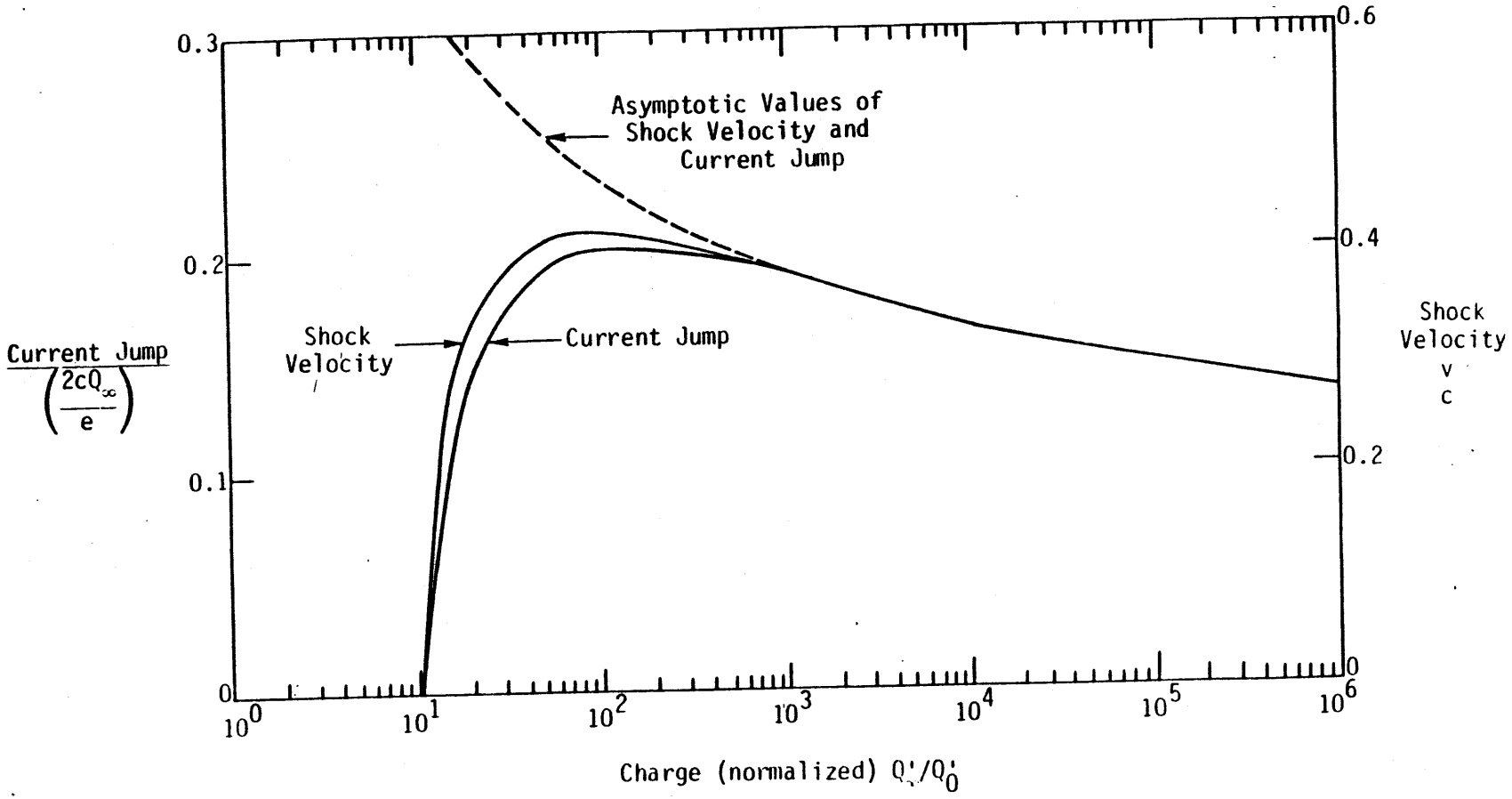

Figure 5. Current and velocity in the limiting case of a step discontinuity ("electromagnetic shockwave") as a function of Q_∞/Q_0. As the current and velocity are proportional in the asymptotic limit, for fixed Q_∞, the same curve gives each.

For $0 < t < t_f$ and zero otherwise. Here t_f is the arrival of the return stroke at the top of the channel. Equation 33 implies that the shock solution does not exist for $Q'_\infty/Q'_0 < 11.96$, at which point the velocity and current fall to zero. See Table 1 for a listing of other Q'_∞/Q'_0 of interest.

We can solve (34) for Q'_∞ in terms of β:

$$Q'_\infty = Q'_0 \, e^{(\beta^{-2})} \tag{39}$$

and relate I and β directly, assuming Q'_0 is fixed:

$$I = \beta c Q_0 e^{(\beta^{-2})} \tag{40}$$

Note that as β increases, I decreases. This is contrary to the results of Wagner [11]. The reason is the lack of dissipation in our shock model. If, following Wagner, we were to assume the dominant loss of energy were to arc formation, and assumed $v(W(\text{ahead}) - W(\text{behind})) = AIv$ where A is a constant, we would still have $v = Ie/Q'_\infty$, but now we would have arc loss dominates in the limit that the radiation losses (see Appendix A):

$$I = \frac{Q_\infty^{3/2}}{e\sqrt{4\pi\epsilon_0 eA}} = \frac{v^3\sqrt{4\pi\epsilon_0 eA}}{e} \tag{41}$$

which accords well with the expressions of [11]. It should at this point be noted that the "field data" referred to by Wagner [11] are <u>not</u> simultaneous measurements of current I and velocity v, but a correlation between them inferred from the separate frequency distributions of I and v for

recorded strokes. Consequently, it is not at all clear that I is really correlated with v as shown. On the other hand, as it is well-known that a lightning return-stroke results in a heated channel (which gives off optical and acoustic emissions as a result). This non-electromagnetic loss of energy should be accounted for in any reasonable model of the return stroke. Furthermore, estimates show that the non-electromagnetic energy losses are typically of the order of 10^6 W/m and exceed the electromagnetic losses by a few orders of magnitude. Consequently, the "lossy shock" model developed here is quite plausible. Indeed, it will be shown that dissipation at the wavefront is a necessary consequence of the equations developed here. Clearly, more observations are needed.

V. MATCHING OF SHOCK AND CONTINUOUS SOLUTIONS

The formal solution (7) of Chen [19] to (3) and (4) develops shock discontinuities in finite time. This is shown below and discussed briefly by Chen [19]. Zeldovich and Raizer [24] discuss the analagous case for a shockwave in a gas, and illustrate the point with fig. 6. The matching of continuous and shock solutions is discussed by Whitham [25].

In general, the solution (6) will have the appearance of the curve ABCDEF of fig. 7. The physical charge distribution must, however, be single-valued. A shock must therefore occur to the right of point B and to the left of D. In general, we will <u>not</u> be able to do this. If $Q'(F) > 0.0836\, Q'_\infty$, no shock can connect any point on FED to the initial state. Even if the above condition were satisfied, a more stringent constraint is that for the shock solution (36-37) to join a continuous solution (18), we need $I_{shock} = I_{continuous}$ for equal Q'. For $Q'_\infty/Q'_0 = 10^3$ this requires $Q'/Q'_\infty \approx 0.02$, for $Q'_\infty/Q'_0 = 10^2$, $Q'/Q'_\infty \approx 0.008$. The solutions to be presented in the next section require shocks which do not satisfy these constraints.

The physical implication of this result is that a dissipative process (e.g., the energy which goes into channel heating, ionization, and radiation) at the shock is required in order to alter the jump (shock) relation $I_{shock}(Q')$ so that it can match to a continuous solution. If we alter the right-hand side of (32) to include a dissipation term $D>0$, we reduce the I_{shock} for a given Q', i.e., we raise the allowable Q' for a given $I_{shock} = I_{continuous}$. We will show in the next paragraph how to obtain the shock location from charge conservation. The shock relation may then be used to infer the dissipation required at the shock front to achieve this.

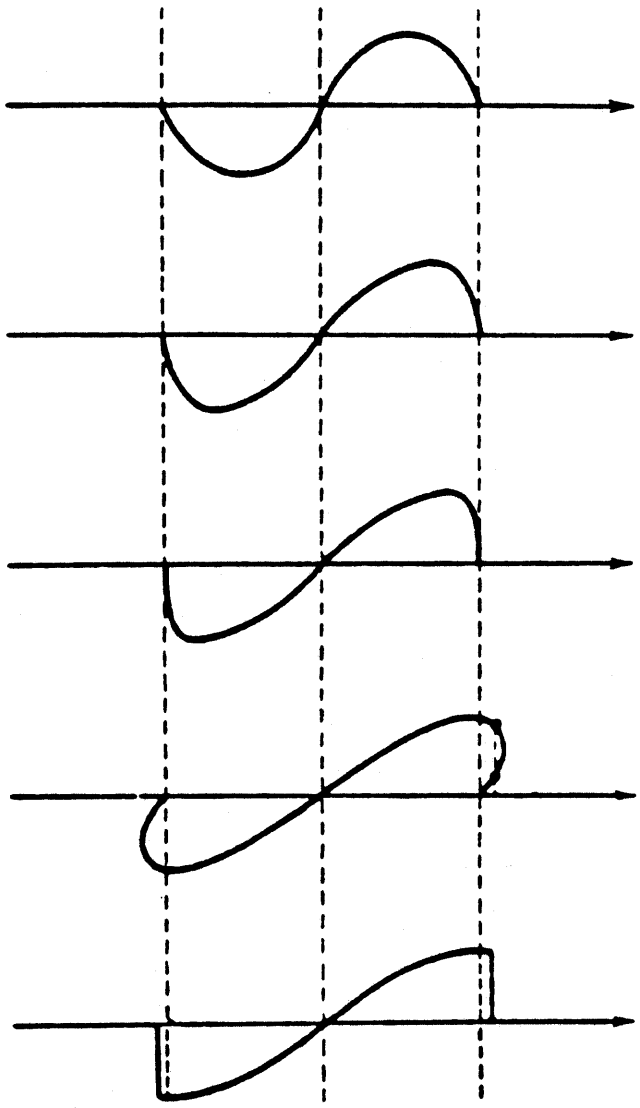

Figure 6. Sketch, from Reference 24, showing the evolution of a shock as a nonmonotic function.

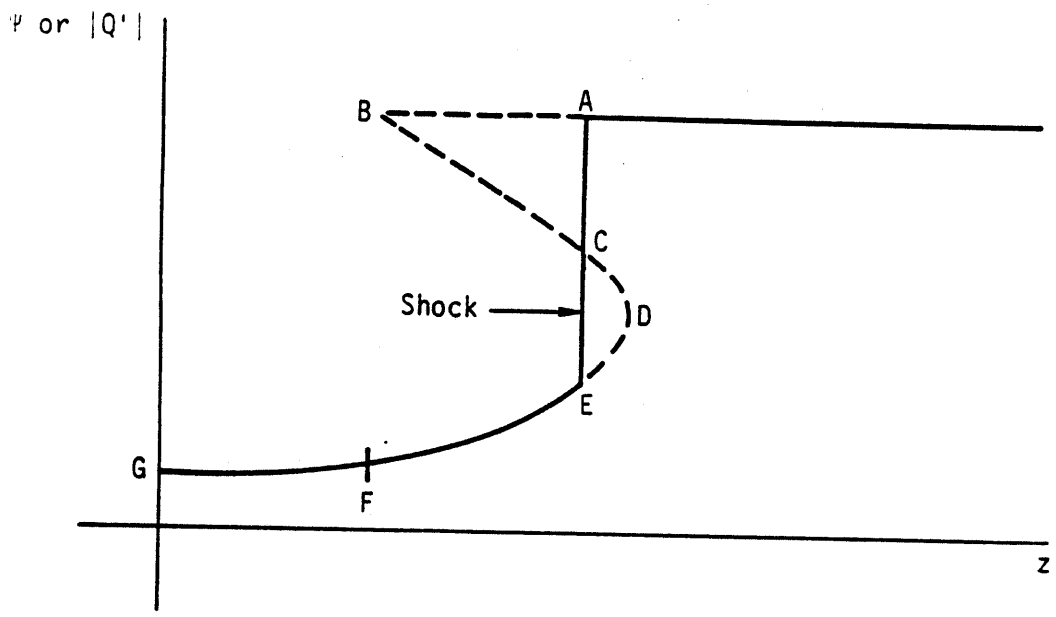

Figure 7. Location of electromagnetic shock.

Note that the infinite value of $\dot{I}$ still leads to a finite radiated signal. See, e.g., Price and Pierce [23] for an example. The corresponding solution is physically reasonable, although the magnitude and time dependence of the dissipation is dependent upon the assumed $Q'(\tau)$ behavior. In principle, one might determine $Q'(\tau)$ for a shock-like wave along a lightning channel by requiring a specified $D(\tau)$ at the front.

The proper shock location may be found as follows. If $Q'(\tau)$ is specified (see the next section for specific examples) then $I(\tau)$ will be determined. As $\tau = t - z/v$, $I(t, z = 0) = I(\tau)$, so the current flowing out of (or into) the half-space $z > 0$ is determined. Given the initial charge in the region $Z > 0$, we know from the time integral of $I(z = 0)$ the total charge in the region at any later time, because charge is conserved. The continuous solution (6) therefore determines the total charge in the region at any time, as it satisfies the boundary condition at $z = 0$ and conserves energy. Any physically correct solution must therefore have the same total

charge for $z > 0$ at the same time as (6). If the continuous solution becomes double-valued, and is therefore physically unacceptable, a "shock" discontinuity may be inserted to achieve a single-valued solution, if, as shown in fig. 7, that shock does not change the total charge of the half-space. Thus, area ABC = area CDE must be used to locate the shock.

The motion of point D in fig. 7 bounds the motion of the shock front. At D, $\partial z/\partial Q' = 0$. This may be recast as

$$z_D = -1/\left[\left(\frac{dQ'}{d\tau}\right)\left(\frac{d}{dQ'}\right)\left(\frac{1}{v}\right)\right]$$

$$= \frac{-2c|Q'|\left[\ell n\left(\frac{Q'_\infty}{e|Q'|}\right)\right]^{3/2}}{\sqrt{\ell n\left(\frac{Q'_\infty}{Q'_0}\right)}\ \frac{dQ'(\tau)}{d\tau}} \qquad (42)$$

This equation is implicit in z, since τ is a function of z, $\tau = t - z/v(Q')$.

VI. AN ILLUSTRATIVE INITIAL VALUE PROBLEM

Consider the moment when the stepped leader first makes electrical contact with the ground (or better, upward propagating leader), resulting in the launching of a return stroke. We may represent this as the interaction at ground level ($z = 0$) of two waves of opposite charge and velocity colliding. This is sketched in fig. 8. The superposition results in a discharge wave propagating upward for $z > 0$ and its image for $z < 0$. The solution of the transmission line equations above (6) leaves arbitrary the functional form of $Q'(\tau)$. Let us consider simple functions for illustrative purposes of the form

$$\begin{aligned} Q'(\tau)/Q'_i &= f + (1 - f)(1 - \tau/\tau_0)^N \qquad 0 < \tau < \tau_0 \\ &= f \qquad \tau > \tau_0 \\ &= 1 \qquad \tau < 0 \end{aligned} \tag{43}$$

where Q'_i is the charge per unit length on the lightning channel, and f is the fractional charge remaining after the wave passes. Here τ has units of time. This functional form for Q' may be interpreted as a time dependence of Q' at ground level of $(1-\tau/\tau_0)^N$, since here the variable τ reduces to t. Note that in the notation of the preceding sections of this paper and of [7], $Q'_0 = fQ'_i$ and $Q'_i = Q'(-\infty)$. We nondimensionalize using τ_0 as our unit of time, with the dimensionless $\tau' = \tau/\tau_0$, giving us the relation for $\tau' = 1 - \{((Q'/Q'_i) - f)/(1 - f)\}^{(1/N)}$. For any position on the lightning channel ($z > 0$): $z = -v(\tau - t)$ where t is time (assumed $t = 0$ at the start of the wave). Normalizing speed by c (and hence distance by c), we have a nondimensional distance $Z = -\beta(\tau' - T)$ where $T = t/\tau_0$, $Z = z/c\tau_0$. When calculated by these formulae, the curves of current and charge on the channel are not single-valued functions, because v is a function of Q and hence τ', so any $z = v(\tau_2)(\tau_2 - t) = -v(\tau_1)(\tau_1 - t)$ may be satisified by $\tau_2 \neq \tau_1$ if for $\tau_2 > \tau_1$, $v_2(\tau_2) < v(\tau_1)$. This ambiguity is resolved as discussed in Section

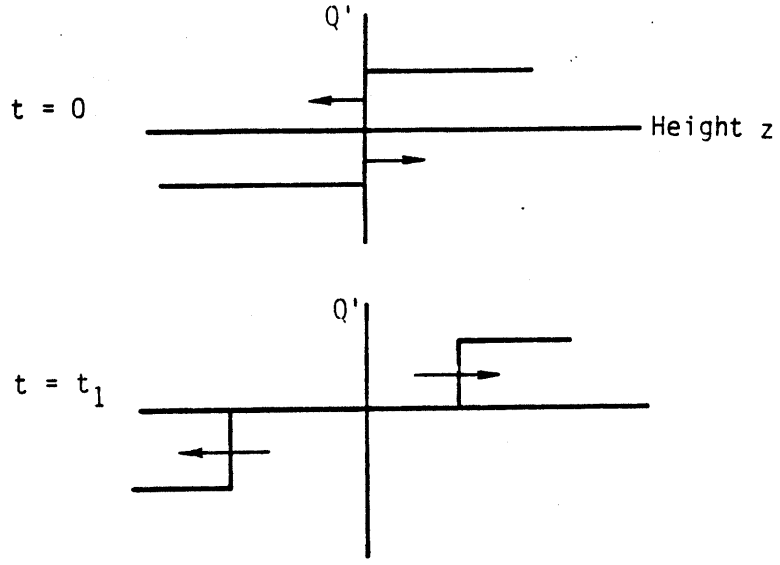

Figure 8. Lightning transmission line viewed as superposition of two oppositely-moving traveling waves. At t = 0 we have a charged line and its image at the ground plane z = 0. At later times we have a portion of the line with charge depleted and its image.

2C above. Rather than compute areas for various choices of front position until equality is achieved, we fit a parabola to the "tip" of the charge profile. With this approximation we can analytically compute the areas and find the shock position which conserves charge. (Of course, none of this is done if the profiles are single-valued.) The figs. 9 through 14 show evolution of the current and charge profiles versus z on the lightning channel, for N = 1,2,3. The distance is scaled by $c\tau_0$ and the curves are at times scaled by τ_0, $T = t/\tau_0$ taking on values from 0.2 to 1. Note that a jump or shock forms, after which the solution is no longer a function and part of the plotted curve is unphysical. Before this singularity, the current peak is behind the shock front, in accord with the comments above about the nonmonotonicity of I(0). This is seen most clearly in figs. 11 and 13.

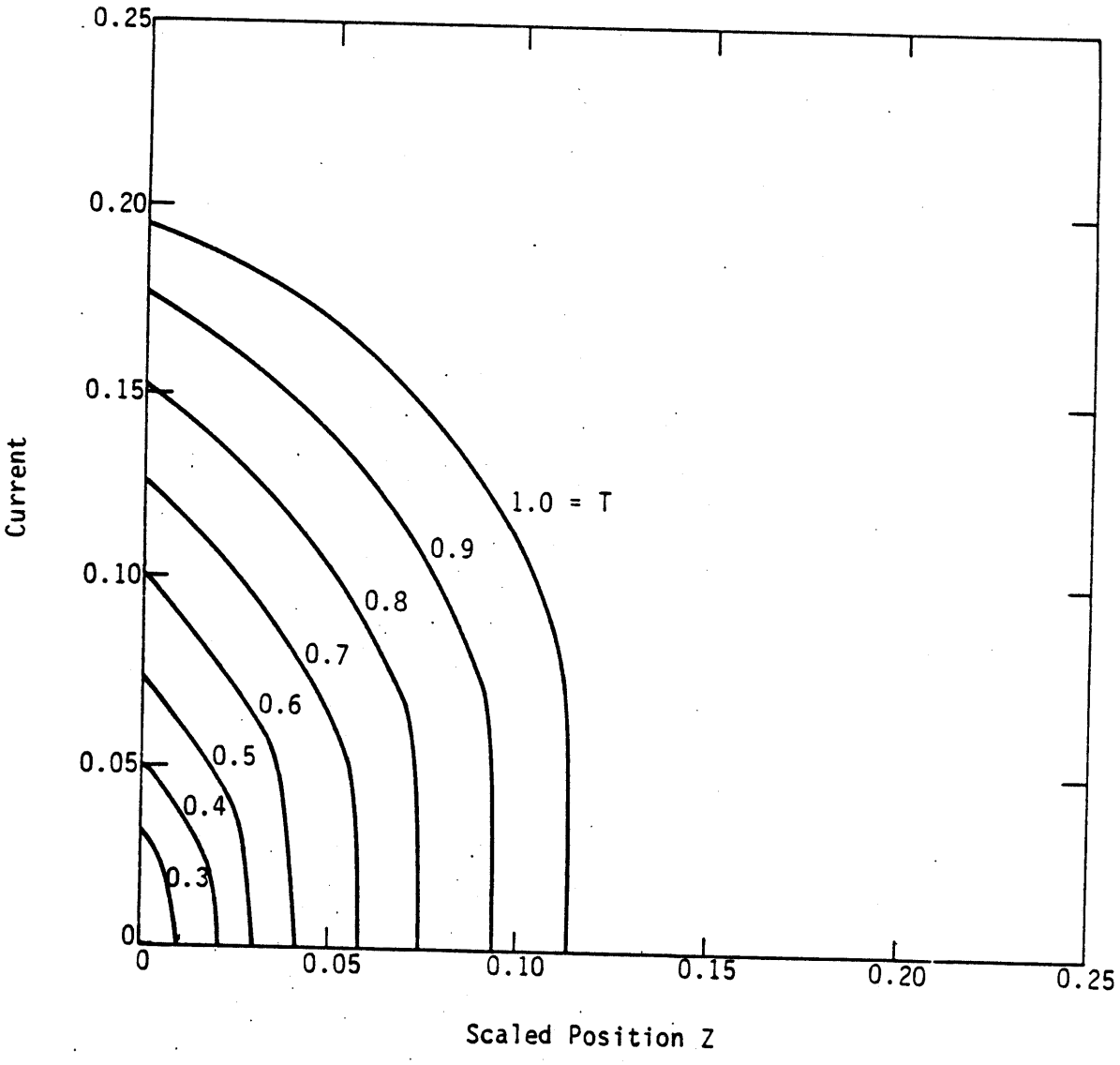

Figure 9. Current versus scaled position Z for N=1. Curves are labeled with scaled time T.

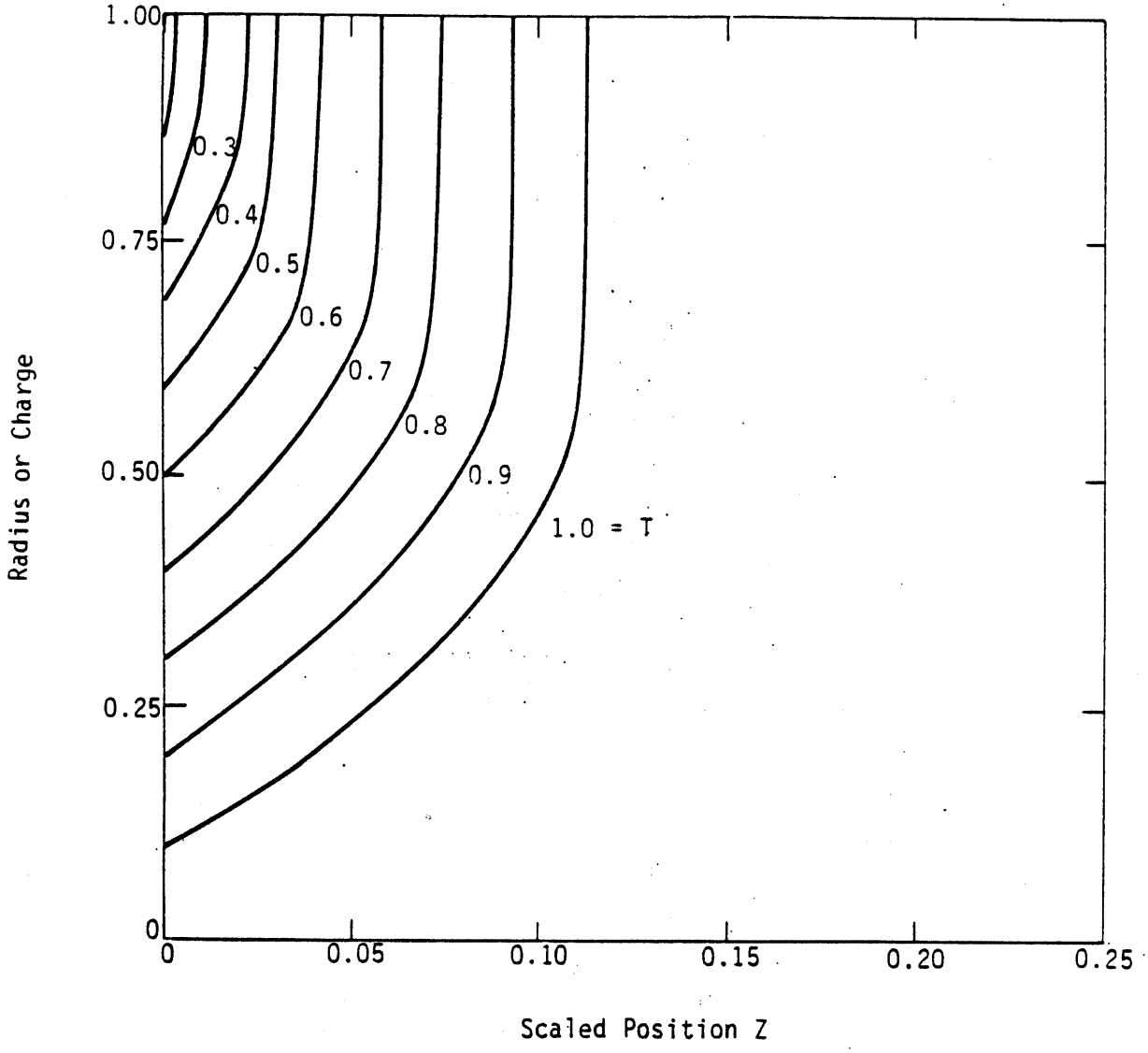

Figure 10. Coronal radius or charge versus scaled position T for N=1. Curves are labeled with scaled time T.

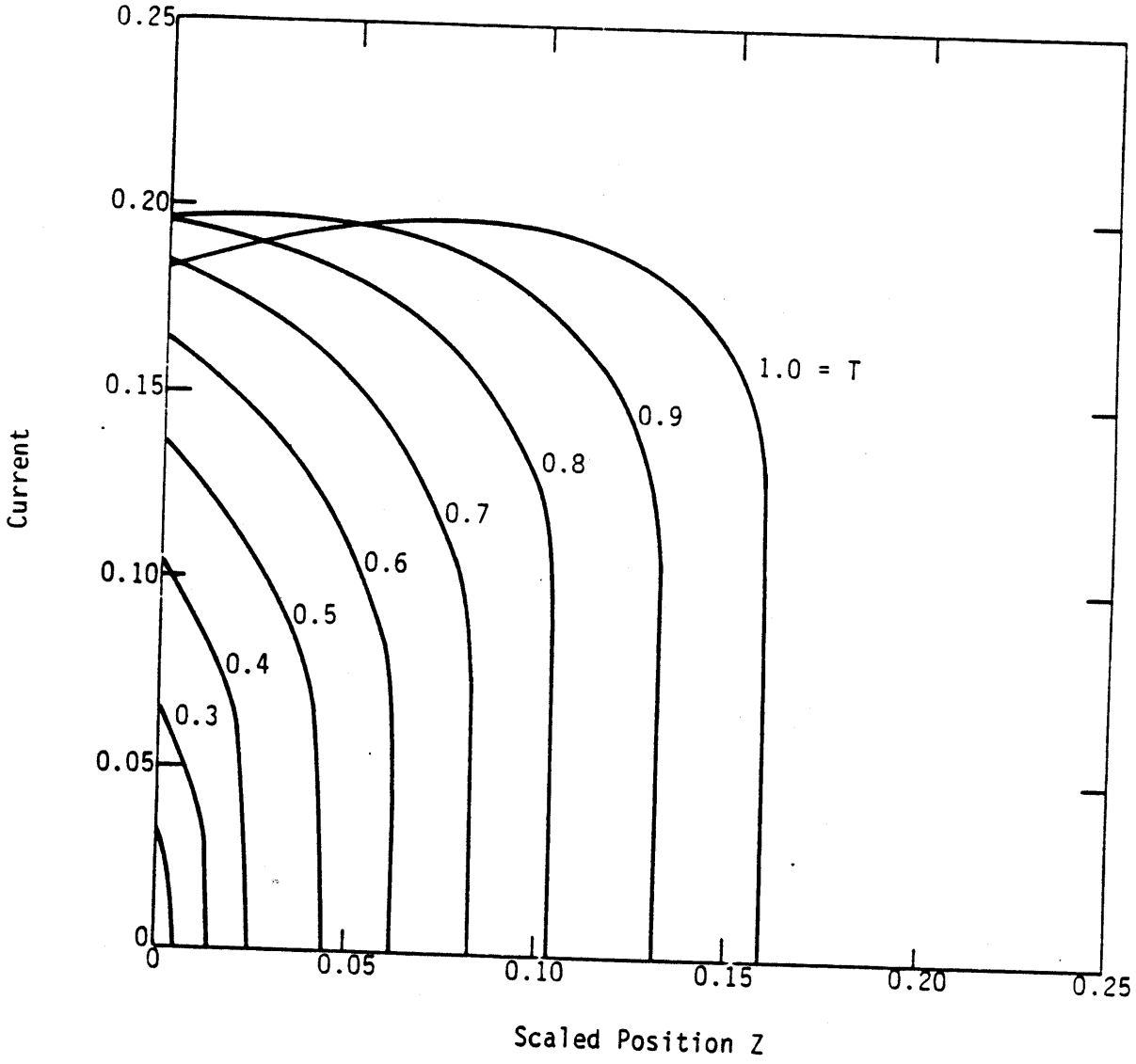

Figure 11. Current versus scaled position Z for N=2. Curves are labeled with scaled time T.

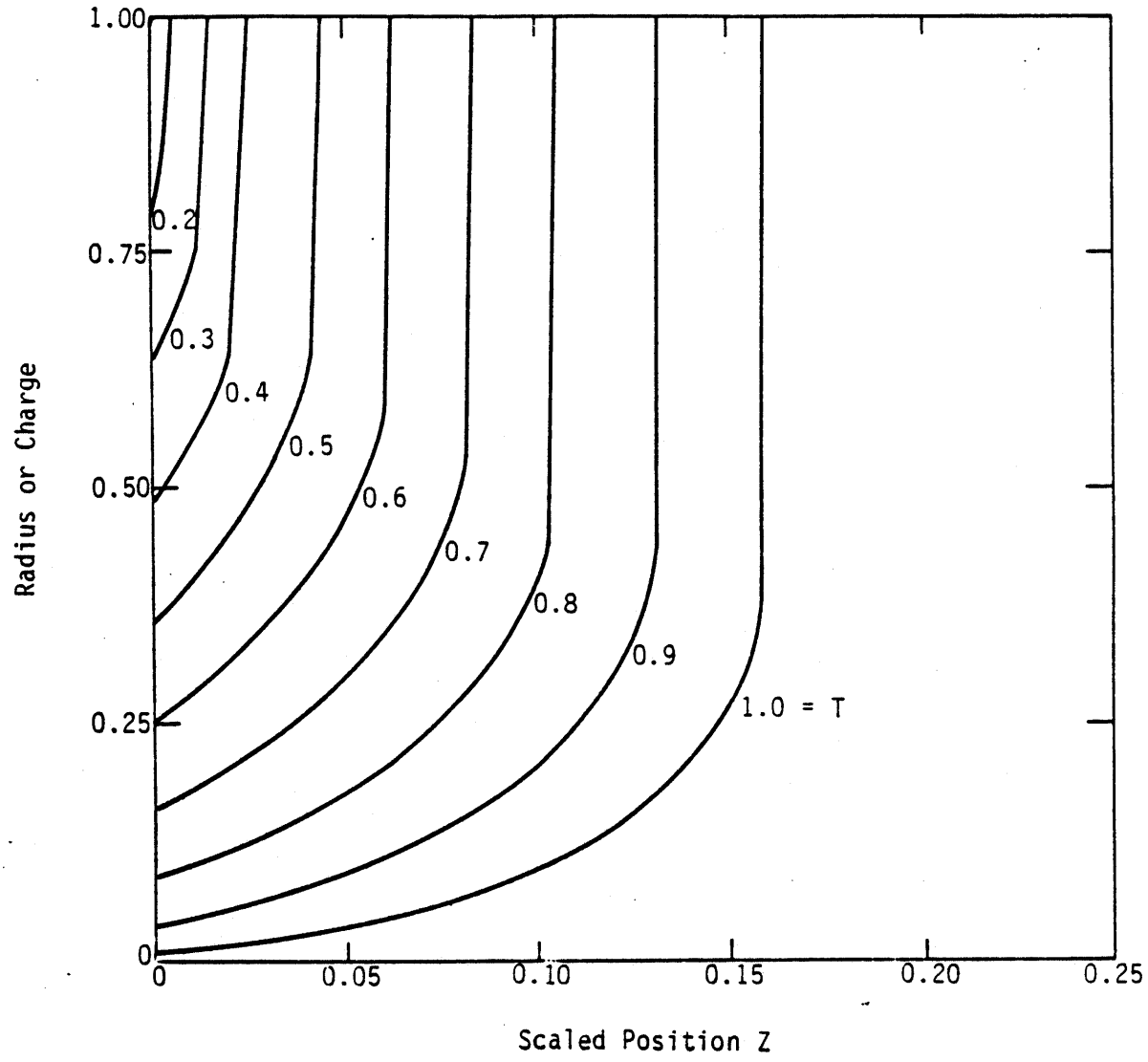

Figure 12. Charge versus scaled position Z for N=2. Curves are labeled with scaled time T.

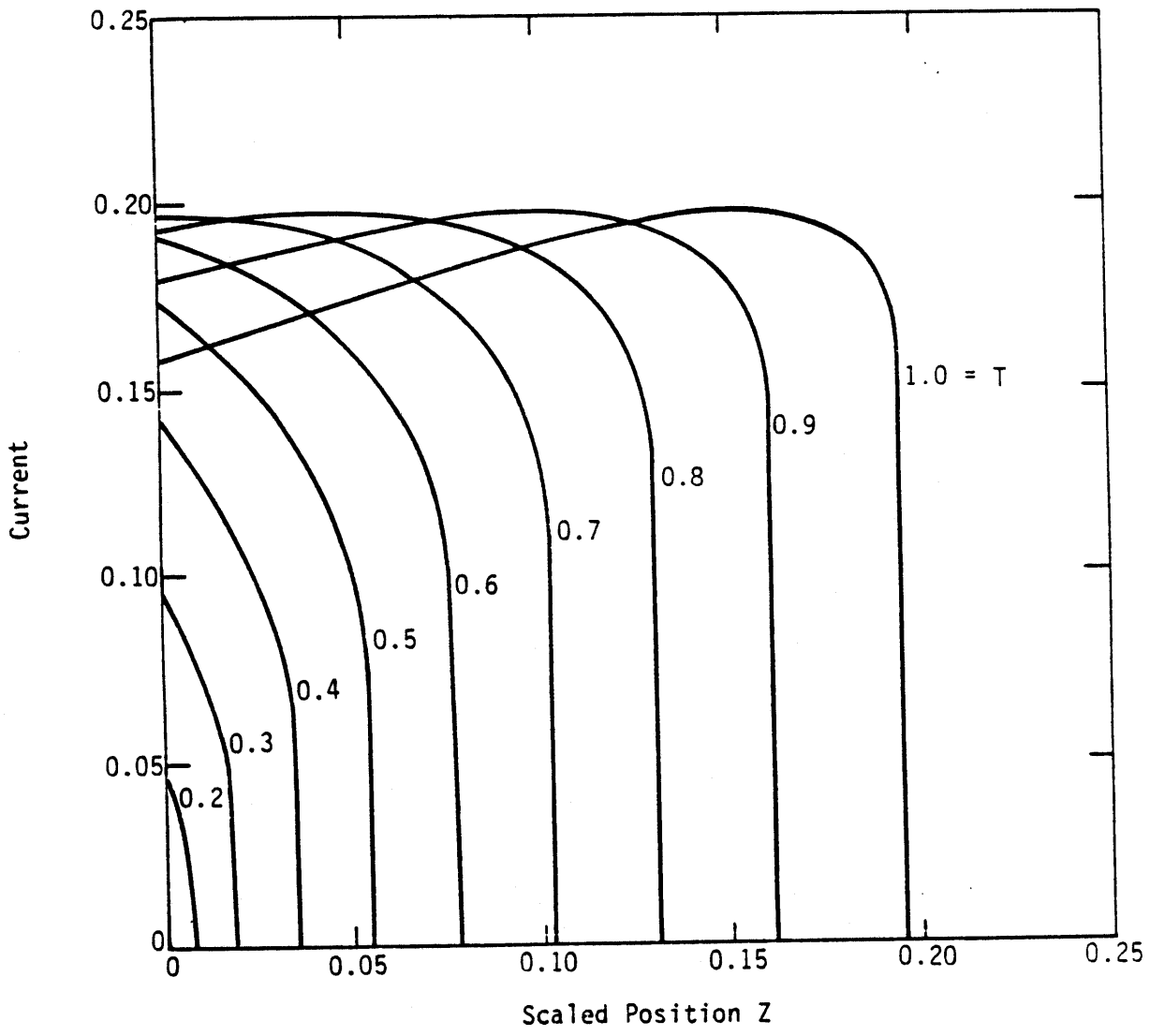

Figure 13. Current versus scaled position Z for N=3. Curves are labeled with scaled time T.

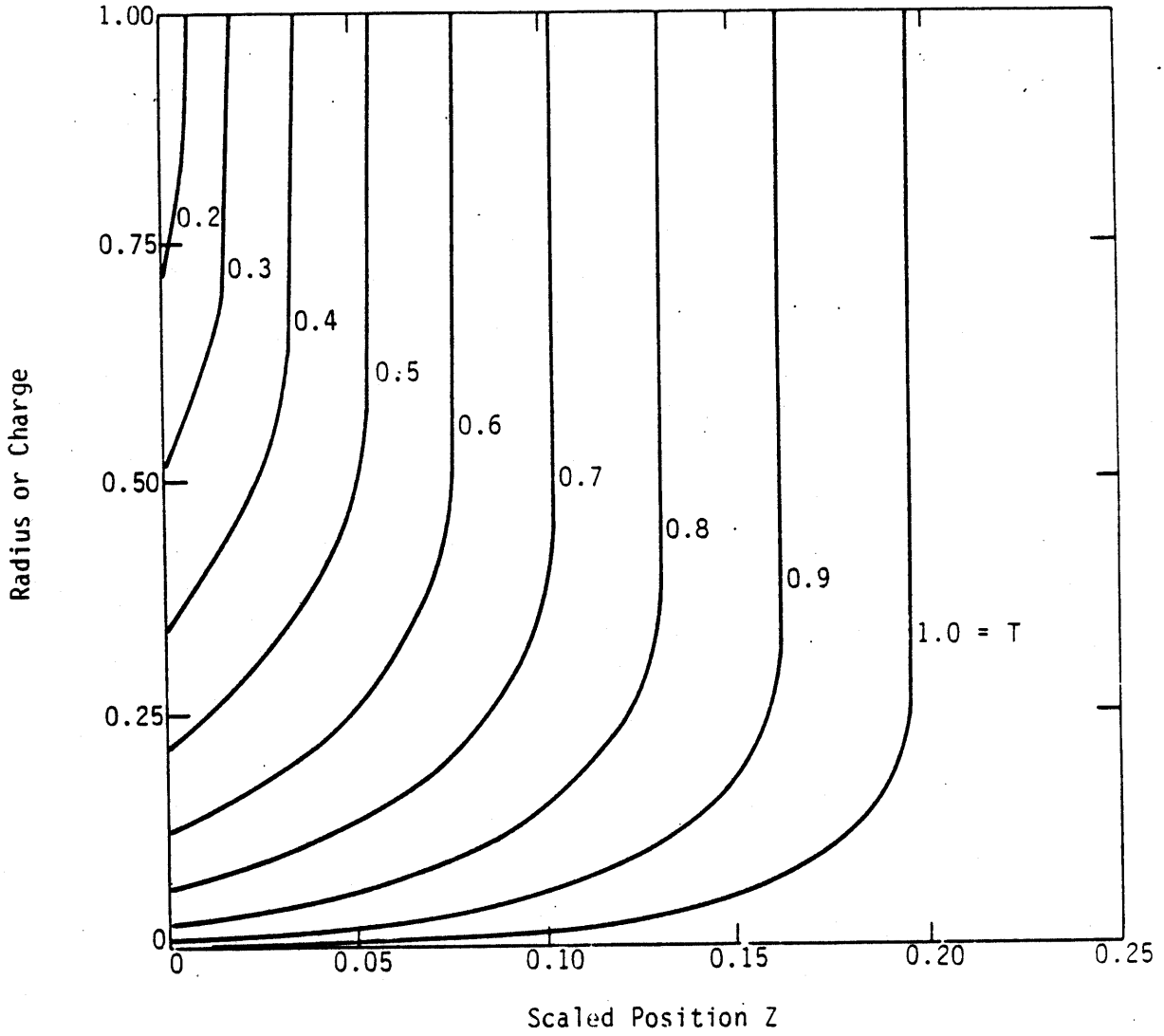

Figure 14. Coronal radius versus scaled position Z for N=3. Curves are labeled with scaled time T.

VII. DISCUSSION

The most significant and testable feature of this model is the prediction of the existence of a corona with a radius of the order of meters. Such a corona should be optically observable. The model explains simply the first return stroke. The subsequent return strokes are possibly the result of the discharge of the channel after a recharging of the corona by the dart leader.

We would warn that electromagnetic signals are probably not well represented by the model, for a number of reasons. Dissipative effects such as channel resistance or the conductance of the corona are neglected. Gardner's model [4] showed a "shallowing" rather than a steepening of the front with propagation, due to channel resistance. The inclusion of non-zero resistance and finite corona conductivity (as due to finite electron drift velocities in the corona) would result in additional dispersive effects on the transmission line, which could counteract the tendency of the front to steepen, and precise values of these parameters would have to be known to predict which tendency would dominate.

Finite drift velocities and conductivities in the corona prevent charge from being depleted instantly at any point, as assumed. This effect alone limits rise time. The charge carriers in the corona cannot move faster than the speed of light. For a 3 m radius corona, this gives a minimum rise time of 10 ns, for example. Collisions will slow the drift velocities and increase rise times further. Collisional processes in the corona give a finite drift velocity and a finite conductance G' to the corona. They would result in a limiting rise time of order C'/G', the RC timescale for the charged corona. This, along with finite channel resistivity can be formally included in the model, but an analytic solution of (6) would no longer hold. At present, we know of no theory of the corona which would permit us to calculate G' accurately. Radiation resistance, i.e., the radiation reaction on the accelerating charged particles, would limit I

even if no collisional dissipation were present. The losses due to electromagnetic radiation are not fully included in this model. (In the shock model, for example, only the axial Poynting flux is accounted for.) While it is not difficult to calculate a radiation resistance using antenna theory, one cannot localize the loss (i.e., find a resistance-per-unit-length distribution along the channel). Consequently, radiation losses cannot be included in a transmission line model in a simple manner.

It is clear that there is room for theoretical and experimental study of coronal phenomena. The studies of [5] and [6] inferred but did not directly observe corona. The inferred corona were of a few centimeters radius, two orders of magnitude smaller than the expected corona radius for lightning. Such a corona might be directly observed with holographic interferometry. A ruby laser used as part of a Mach-Zehnder interferometry would give electron number density through the usual Abel-inversion of the fringe shift as a function of radius. Such information would be valuable since the references cited note discrepancies between inferred coronal radius and that expected from equivalance of (5). In fact, [5] suggests such a model underestimates the coronal radius, while [6] suggests it overestimates the radius. Direct measurement of charge densities, as discussed above, could clear this up and pave the way for a theory of coronal discharges which include time-dependence and nonideal effects such as finite drift velocities.

It is well known [27] that the linear telegrapher's equations combine the features of the wave and diffusion equations, which are different limits for the equation. In general, we have a finite front propagation velocity (as in the wave equation and unlike the parabolic diffusion equation which can transmit signals with infinite velocity) with a signal that is smoothing out. To illustrate this, we have solved the case of a transmission line with a current pulse at one end with time dependence $(1-\exp(-at))$. This is analytically solvable by Laplace transforms if $a = R'/L'$ for the transmission line, with the conductance per unit length $G' = 0$. The solution may be put in the form of the convolution:

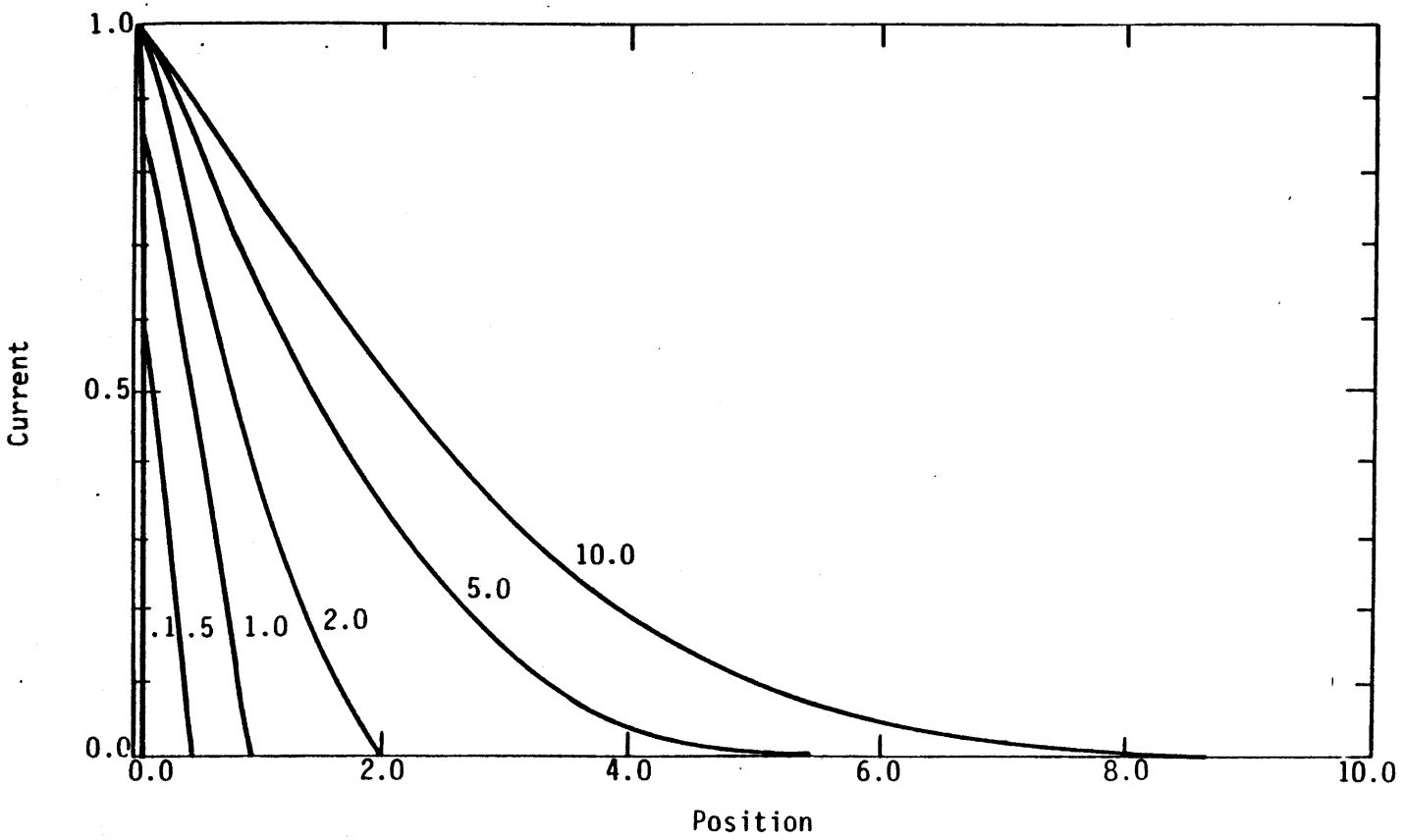

Figure 15. Wave propagation along a transmission line with dissipation, illustrating the diffusive nature of the propagation introduced by finite resistance. The nondimensional times T are shown for each curve.

$$f(T,q) = 2e^{-T} \int_0^y dx\, I_0(T - x)\, I_0(x^2 - q^2)\, u(x - q) \qquad (44)$$

where $T = at/2$ is a nondimensional time, $q = az/2v$ a nondimensional distance (with v the wave velocity along the line, $v = 1/(L'C')^{1/2}$), u the unit step function, I_0 the modified Bessel function. The solution is plotted in fig. 15 for nondimensionalized times T = 0.1, 0.5, 1.0, 2.0, 5.0, and 10. Note the reduction of gradients near the front as a function of time. We expect on the basis of this behavior of the telegrapher's equation that dissipative effects such as finite conductivity of the channel or the corona would tend to prevent shock formation. We note further from the figure that while the edge of the front moves at v, the velocity of any finite value slows with propagation (e.g., note that the position of half of full current has moved roughly the same distance in the time interval 5-10 as in the interval 2-5). This confirms the results of Gardner [4]. For general inverse rise time constants a not equal to the transmission line R'/L', the solution cannot be written so simply as a convolution integral, but the qualitative effect of finite resistivity should be the same. Webster [25] presents an example of an impulsive application of a fixed voltage V to a line with resistance. There is in this case, due to the infinite rise time of the driving pulse, a step discontinuity at the wavefront, which decreases in magnitude expontially with time as it propagates: it is very much like a diffusion wave for $z < vt$ but with zero intensity for $z > vt$,and a sharp transition at the front $z = vt$. For finite values of the time derivative of I, we would not have this discontinuity. In principle, a model similar to Gardner's but embodying channel parameters modified by the existence of a corona could be used to study such effects, including the nonlinearity introduced by the dependence of the capacitance per unit length on Q'. In addition to finite resistance, variable inductance per unit length due to channel expansion could also be included in a numerical model.

As discussed above, the inductance, which is modeled here as a constant, would actually be frequency-dependent, giving rise to a dispersion

not accounted for in this simple model. In this context the sensitivity of the corona radius to return current radius for fixed front velocity should be noted. Physically, the coronal radius should therefore be determined by the dominant frequency component of the current distribution. Uncertainty of the parameters such as channel radius, and breakdown electric field (or, equivalently, corona radius) make quantitative predictions of wave velocity, etc. difficult. It seems clear that a more detailed, dynamic corona model is needed for accurate prediction of corona radius. A more sophisticated treatment would seem to be called for, especially if observations reveal a corona as this model suggests. Nonideal transmission line properties and coronal physics could impose limitations on how rapidly charge could be drained from the corona, limiting current rise and fall times.

In conclusion, this model successfully explains many features of return strokes, including 1) the amount of charge transfered in return strokes 2) the approximate equality of charge transfered by return stroke and continuing current. It makes testable predictions, most notably about the effects of a corona discharge with a radius of the order of 1-10 m, which should be observable.

REFERENCES

1. M. A. Uman, in Planetary Electrodynamics, (Hughes and Coroniti, ed.) Gordon and Breach, 1969.

2. C. F. Wagner, "Lightning and Transmission Lines," J. Franklin Inst. 283, 558-594, 1967.

3. P. F. Little, "Transmission Line Representation of a Lightning Return Stroke," J. Phys. D. 11, 1893-1910, 1978.

4. R. L. Gardner, A Model of the Lightning Return Stroke, Doctoral Thesis, U. of Colorado, 1980.

5. P. S. Book and H. J. Price, Transmission Line Corona Experiment, Interaction Note 313, 1976.

6. P. S. Book, Study of Corona in a Transmission Line Test Facility, Interaction Note 369, 1978.

7. C. E. Baum, Properties of Lightning-Leader Pulses, Lightning Phenomenology Notes 2, 1981, and Proc. Int'l Aerospace Conference on Lightning and Static Electricity, Oxford, March 1982, paper A6.

8. T. R. Connor, Stroke- and Space-Resolved Slit Spectra of Lightning, Los Alamos Scientific Laboratory Report LA-3754 Addendum, 1968.

9. M. A. Uman, Lightning, McGraw-Hill, New York, 1969.

10. L. E. Salonave, Lightning and Its Spectrum, University of Arizona Press, pp. 117ff, Tucson, AZ, 1980.

11. C. F. Wagner, AIEE 82, p. 609-17 1963.

12. K. Berger, in Lightning, R. H. Golde, ed., Academic Press, London, p. 119, 1977.

13. C. F. Wagner and A. R. Hileman, "The Lightning Stroke-II," Trans. AIEE, 80, 622-642, 1961.

14. E. T. Pierce, in Recent Advances in Atmospheric Electricity, ed L. G. Smith, Pergamon Press, New York, 1958.

15. M. Rao and H. Bhattacharya, "Lateral Corona Currents from the Return Stroke Channel and the Slow Field Change After the Return Stroke in a Lightning Discharge," J. Geophys. Res., 71, 2811-2814, 1966.

16. Uman, op.cit., Ref. 9, p.4.

17. Garbagnati, E., et al, "Pilievi delle cavaltevishiche dei felmine" in Italia. Risulate otteruti negli anni, 1970-1973.

REFERENCES (Concluded)

18. S.A. Schelkunoff and H. J Friis, Antennas: Theory and Practice, John Wiley, New York, p. 236ff, 1952.

19. K. C. Chen, "Transient Corona Effects on a Wire Over the Ground," in Lightning Technology, NASA Conference Publication 2128, 22 April 1980.

20. M. Abramowitz and J. Stegun, Handbook of Mathematical Functions, NBS Monograph #55, U.S. Government Printing Office, 1964.

21. C. E. Baum et. al., Measurements of Electromagnetic Properties of Lightning with 10 nanosecond Resolution (Revised), Lightning Phenomenology Note 3, February 1982. This is an expanded version (more data) of an earlier version (same title, authors) in Proc. Symposium on Lightning Technology, NASA Conf. Pub. 2128, FAA-RD-80-30, April 1980, pp. 39-82.

22. R. Becker, Electromagnetic Fields and Interactions, Dover, New York, Section 68, p. 287, 1964.

23. G. H. Price and E. T. Pierce, Radio Science, 12,, 381 (1977).

24. Ya. B. Zeldovich and Yu. P. Raizer, The Physics of Shockwaves and High Temperature Phenomena, Academic Press, New York, 1966.

25. G. B. Whitham, Linear and Nonlinear Waves, J. Wiley, New York, 1974.

26. Uman, op. cit., p. 133 following Dennis and Pierce, J. Res. NB8 68D (Radio Science), p. 777-794, 1964.

27. A. G. Webster, Partial Differential Equations of Mathematical Physics, Dover, New York, 1945.

28. K. Berger, R. B. Anderson, and H. Kroninger, "Parameters of Lighting Flashes," Electra, Vol. 40, pp. 101-119, 1975.

APPENDIX A
SHOCK WITH DISSIPATIVE FRONT

We derive (38), the relationship between current and velocity, for a shock with an energy loss to arc heating of the form AIv, where A is a constant. This is the form postulated by Wagner [13]. The energy balance is

$$AIv + P = v(U_1 - U_2) \tag{45}$$

Let us consider the limit where this loss dominates the Poynting vector losses (radiation losses). The n

$$IAv4\pi = \left(Q_\infty'^2/\varepsilon_0 e^2 - \mu_0 I^2 \ell n\left(\frac{Q_\infty'}{Q_0'}\right)\right) \tag{46}$$

Eliminating v using $I/v = Q_\infty'/e$ we have:

$$I = \frac{Q_\infty'}{e}\left(4\pi\varepsilon_0 eA/Q_\infty' + \ell n\left(\frac{Q_\infty'}{Q_0}\right)/c^2\right)^{-1/2} \tag{47}$$

This is approximately

$$I \sim \frac{Q_\infty'^{3/2}}{e\sqrt{4\pi\varepsilon_0 eA}} \tag{48}$$

while

$$v = \frac{I}{Q_\infty'} = \frac{Q_\infty^{1/2}}{\sqrt{4\pi\varepsilon_0 eA}} \tag{49}$$

Therefore, the relationship between I and v is found by eliminating Q'_∞:

$$I \sim v^3 \sqrt{4\pi\varepsilon_0 eA}/e \tag{50}$$

which is (38).